Proc. Natl. Acad. Sci. USA
Vol. 94, pp. 5012–5017, May 1997
Biochemistry

The dTTPase mechanism of T7 DNA helicase resembles the binding change mechanism of the F_1-ATPase

MANJU M. HINGORANI, M. TODD WASHINGTON, KRISTEN C. MOORE, AND SMITA S. PATEL*

Department of Biochemistry, Ohio State University, 484 West 12th Avenue, Columbus, OH 43210

Communicated by F. William Studier, Brookhaven National Laboratory, Upton, NY, March 17, 1997 (received for review December 19, 1996)

ABSTRACT **Bacteriophage T7 DNA helicase is a ring-shaped hexamer that catalyzes duplex DNA unwinding using dTTP hydrolysis as an energy source. Of the six potential nucleotide binding sites on the hexamer, we have found that three are noncatalytic sites and three are catalytic sites. The noncatalytic sites bind nucleotides with a high affinity, but dTTPs bound to these sites do not dissociate or hydrolyze through many dTTPase turnovers at the catalytic sites. The catalytic sites show strong cooperativity which leads to sequential binding and hydrolysis of dTTP. The elucidated dTTPase mechanism of the catalytic sites of T7 helicase is remarkably similar to the binding change mechanism of the ATP synthase. Based on the similarity, a general mechanism for hexameric helicases is proposed. In this mechanism, an F_1-ATPase-like rotational movement around the single-stranded DNA, which is bound through the central hole of the hexamer, is proposed to lead to unidirectional translocation along single-stranded DNA and duplex DNA unwinding.**

Helicases are emerging as a class of energy transducing ATPases whose function is to unwind double-stranded DNA (dsDNA) to single-stranded DNAs (ssDNA) (1–4). Helicases are analogous to motor proteins such as myosin, kinesin, and dynein that use ATP hydrolysis to perform work. The mechanism of energy transduction in helicases and in motor proteins is a subject of intense study that will require both knowledge of the high-resolution structure of the protein and elucidation of the enzyme kinetics. Recently the x-ray crystal structure of a DNA helicase from *Bacillus stearothermophilus* was solved (5). This structure is of the monomeric form of the enzyme without DNA bound to the protein. Thus one awaits the high-resolution structure of the active oligomeric form of a helicase, which will provide a better understanding of the cooperativity and coordination in catalysis among the oligomeric subunits that is critical for the action of helicases.

4A′ protein, the subject of this study, is a 63-kDa product of T7 gene 4 that provides the helicase and primase activities necessary for bacteriophage T7 DNA replication (6). 4A′ is a ring-shaped hexameric helicase that binds ssDNA through the central hole (7, 8). DNA binding is modulated by the state of the nucleotide bound to the hexamer. Tight DNA interactions are observed in the presence of nucleoside triphosphate, preferably dTTP or its nonhydrolyzable analog dTMP-PCP (β-γ-methylene deoxythymidine triphosphate) and these interactions are weaker in the presence of dTDP (9). Thus, dTTP binding and hydrolysis can function as switches that promote DNA binding and release—steps necessary for translocation of the helicase on the DNA.

Several reports in the literature have suggested structural similarities between helicases, recA, and the F_1-ATPase particle of the ATP synthase complex. For example, although rho and F_1-ATPase enzymes are involved in very different processes, the two share considerable amount of amino acid and secondary structure homology (10, 11). The predicted structures of 4A′ and *Escherichia coli* rho helicases, based on mutagenesis results (10, 12), show similarities to the nucleotide binding domains of F_1-ATPase and recA (11, 13). The recently determined three dimensional structure of PcrA helicase (5) also shows that its nucleotide binding subdomain is homologous to that of recA and F_1-ATPase. In addition, recently Yu and Egelman (14) have modeled a high resolution structure of recA hexamer, which usually adopts a helical filament structure. This structure of the recA ring is similar to the structure of the F_1-ATPase $\alpha_3\beta_3$ ring and it was suggested to be a model for the structure of hexameric helicases. Although it is likely that helicases are structurally similar to the F_1-ATPase, no mechanistic similarities have been reported.

The nucleotide binding and pre-steady-state dTTPase kinetic experiments, described in this paper, suggest mechanistic similarities between 4A′ and F_1-ATPase. The two enzymes are structurally similar as outlined above, and our studies show that, similar to F_1-ATPase, 4A′ hexamer also has noncatalytic and catalytic nucleotide binding sites. The catalytic sites show strong cooperativity which leads to sequential binding and hydrolysis of dTTP. The elucidated dTTPase mechanism of 4A′ is remarkably similar to the binding change mechanism of the ATP synthase. To our knowledge, the findings reported here are the first mechanistic similarities found between these two systems. This will represent an important step in understanding the helicase function because of the wealth of structural, kinetic, and mechanistic data available for the F_1-ATPase. In this report, we compare the mechanisms of these two systems and suggest that to translocate along ssDNA, 4A′ may use a rotation-linked catalysis similar to that of the F_1-ATPase.

MATERIALS AND METHODS

Protein Purification. The 4A′ protein was purified to homogeneity and stored as described (15, 16). The protein concentrations were determined both by absorbance measurement at 280 nm in 8 M urea (the extinction coefficient is 76,100 $M^{-1}\cdot cm^{-1}$) and by Bradford assay using BSA as the standard. Both methods provided similar protein concentrations values. The ability to form stable hexamers was determined for each batch of 4A′ using HPLC gel-filtration experiments in the presence of dTTP (16). These assays showed that nearly 100% of 4A′ formed hexamers (data not shown). Each batch of protein was found to be fully active when tested for active site concentration by DNA binding titrations with the 30-mer DNA that binds with a stoichiometry of one DNA per hexamer (9).

The publication costs of this article were defrayed in part by page charge payment. This article must therefore be hereby marked "*advertisement*" in accordance with 18 U.S.C. §1734 solely to indicate this fact.

0027-8424/97/945012-6$2.00/0
PNAS is available online at **http://www.pnas.org**.

Abbreviations: dsDNA, double-stranded DNA; ssDNA, single-stranded DNA; NC, nitrocellulose.

*To whom reprint requests should be addressed. e-mail: Patel.85@osu.edu.

Nitrocellulose (NC) Filter Binding and Nucleotide Exchange Experiments. [α-^{32}P]dTTP was purchased from Amersham, and its purity was checked and corrected in all the experiments. All the nucleotide exchange experiments were carried out in an 18°C room. 4A′ was mixed with [α-^{32}P]dTTP for 30 s (in 50 mM Tris acetate, pH 7.5/40 mM sodium acetate/10 mM magnesium acetate/10% glycerol) and then chased with nonradiolabeled dTTP (10 mM in the same buffer as above). After varying periods of incubation with the chase, 10–15 μl aliquots were filtered through prewetted NC filters, as described (16). [α-^{32}P]dTMP-PCP was enzymatically synthesized as described (16). The state of nucleotides bound to 4A′ was identified by extracting the NC membranes with 1 M perchloric acid, neutralizing with 0.25 M Tris/1 M NaOH, and analyzing the extracted nucleotides by polyethyleneimine-cellulose TLC.

Pre-Steady-State Kinetic Experiments. These experiments were carried out using a rapid chemical-quench-flow instrument (17) (KinTek, State College, PA). A total of 15 μl of 4A′ at a desired concentration in 50 mM Tris-acetate (pH 7.5), 40 mM sodium acetate, 1 mM DTT, 10% glycerol, and 1 mM magnesium acetate was mixed with 15 μl mixture of dTTP (Sigma) and [α-^{32}P] dTTP (20 μCi per 10 reaction points; 1 Ci = 37 GBq; Amersham or ICN) prepared in the same buffer except with 19 mM magnesium acetate. The reactions were stopped with 1 M HCl, treated with chloroform, and neutralized. The quenched reactions were analyzed by polyethyleneimine-cellulose TLC and the products were quantitated using a PhosphorImager (Molecular Dynamics). In the pulse–chase experiments, after varying reaction times, 0.2 M EDTA or excess nonradiolabeled dTTP in the above buffer with 15 mM magnesium acetate was added from the third syringe in the quench-flow apparatus. After chasing with dTTP for 30 s, the reactions were acid-quenched and analyzed as described above. After chasing with EDTA, the reactions were kept on ice prior to analysis by TLC. Both dTTP chase and EDTA chase experiments gave the same results. The resulting acid-quench and pulse–chase kinetics data were fit using nonlinear regression analysis (KALEIDAGRAPH; Synergy Software, Reading PA).

The Three-Syringe Rapid Chemical Quench Flow Experiment. This experiment was conducted using two delay times (KinTek RQF-3 software). During the first delay time, 4A′ was incubated with [α-^{32}P]dTTP. During the second delay time, unlabeled dTTP was added from the third syringe, and the mixture was held at a constant temperature for times ranging from 10 s to 60 s prior to quenching with 1 M HCl.

RESULTS AND DISCUSSION

The Hexamer Hydrolyzes One dTTP at a Time. To elucidate the mechanism of the dTTPase activity of 4A′ hexamer, we have investigated the pre-steady-state kinetics of dTTP hydrolysis in the absence of DNA. Most of the experiments were carried out at 0.83–5 μM 4A′ (hexamer concentration). At these concentrations, as shown previously (16), 4A′ forms stable hexamers in the presence of dTTP.

The pre-steady-state kinetics of dTTP hydrolysis were measured by mixing 4A′ protein with [α-^{32}P]dTTP in a rapid chemical quench-flow apparatus (17), and stopping the reactions with HCl after millisecond to several second time intervals (see *Materials and Methods*). The resulting acid-quenched kinetics showed a pre-steady-state burst of dTTP hydrolysis (Fig. 1*A*)—i.e. dTTP hydrolysis in the first turnover was faster than subsequent turnovers. The acid-quenched kinetics were measured at increasing [dTTP]. The observed burst rate constant (the fast phase) increased with [dTTP] in a hyperbolic manner (Fig. 1*B*) and achieved a maximum rate constant of 0.66 ± 0.083 s^{-1} with $K_{1/2}$ at 167 ± 57 μM dTTP. The dTTPase turnover rate constant (the linear phase) remained constant in this range of [dTTP] at about 0.04–0.06 s^{-1}. The pre-steady-state burst amplitude also remained constant at an average value of 1.11 ± 0.26 sites per hexamer (Fig. 1*B*). These results show that the 4A′ hexamer hydrolyzes only one dTTP at a rate constant faster than dTTPase turnover.

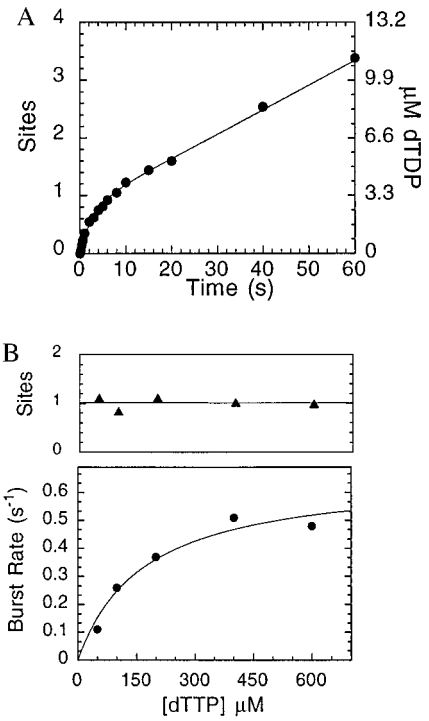

FIG. 1. Pre-steady-state acid-quenched kinetics of dTTP hydrolysis. 4A′ (3.3 μM hexamer) was mixed with [α-^{32}P]dTTP (50–600 μM) in a rapid quench-flow instrument at 18°C, and reactions were quenched with 1 M HCl. (*A*) Representative dTTPase time course at 100 μM dTTP (●) is shown. The data were fit to a single exponential followed by a linear phase with a burst amplitude of 0.80 ± 0.04 dTTP per hexamer, a burst rate constant of 0.34 ± 0.04 s^{-1}, and a dTTPase turnover rate of 0.043 ± 0.0007 s^{-1}. (*B*) The [dTTP] dependence of the burst amplitude (▲) and the burst rate constant (●) is shown. The [dTTP] dependence of the burst rate constant fit to a hyberbola with a maximum dTTP hydrolysis rate constant of 0.66 ± 0.083 s^{-1} and $K_{1/2}$ of 167 ± 57 μM.

Pulse–chase experiments were conducted to determine how many dTTPs were tightly bound to the hexamer prior to hydrolysis and to investigate in greater detail the kinetics of dTTP binding to 4A′. In these experiments, 4A′ was mixed with [α-^{32}P]dTTP for varying times, after which excess nonradiolabeled dTTP or EDTA was added as a chase (see *Materials and Methods*). The dTTP-chased reactions were incubated for an additional 30-s time period prior to acid-quenching. The 30-s chase period allowed any tightly bound [α-^{32}P]dTTP to be converted to [α-^{32}P]dTDP. Thus, the kinetics of dTDP formation in the pulse–chase experiments measure both the rate constant of dTTP binding to 4A′ and the number of dTTPs tightly bound prior to hydrolysis. Similar to the acid-quenched kinetics, the pulse–chase kinetics (Fig. 2*A*) also showed a pre-steady-state burst of dTTP hydrolysis. However, unlike the acid-quench burst amplitude of one dTTP per hexamer, the pulse–chase burst amplitude corresponded to 2 dTTPs per hexamer.

Closer examination of the pulse–chase kinetics showed that the tight binding of the two dTTPs to 4A′ occurs at different times. This was inferred from the fact that the pulse–chase burst kinetics fit best to two exponentials (Fig. 2*A*). The exponential rate constant of the fast phase increased linearly with [dTTP] (Fig. 2*B*), thus the measured slope and intercept provided, respectively, the apparent bimolecular rate constant

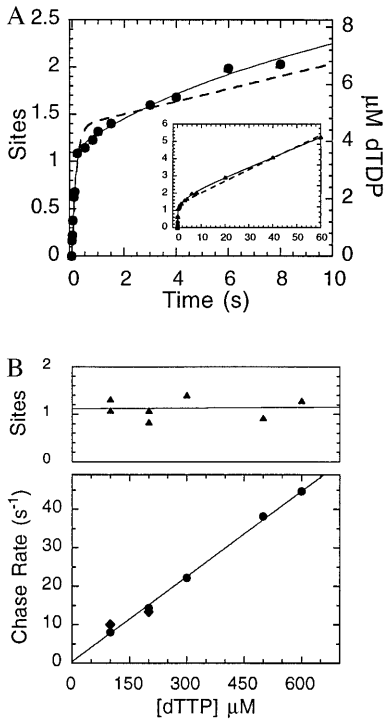

FIG. 2. Pre-steady-state pulse–chase kinetics of dTTP hydrolysis. 4A′ (3.3 μM hexamer) was mixed with [α-^{32}P]dTTP (100–600 μM) in a rapid quench-flow instrument at 18°C, and the reactions were chased with dTTP or EDTA (see *Materials and Methods*). (*A*) Representative time course of the pulse–chase kinetics at 100 μM dTTP is shown. (*Inset*) The entire pulse–chase time course to 60 s. The pulse–chase kinetics fit best to two exponentials (solid line) followed by a linear phase. The first phase amplitude is 1.09 ± 0.05 dTTP per hexamer, fast exponential rate constant is 10.0 ± 1.1 s^{-1}, second phase amplitude is 0.61 ± 0.07 dTTP per hexamer, second exponential rate constant is 0.23 ± 0.07 s^{-1}, and steady-state dTTPase turnover is 0.06 ± 0.002 s^{-1}. The dotted line shows the poor fit to one exponential followed by a linear equation. (*B*) The [dTTP] dependence of the first phase amplitude (▲) and rate constant [EDTA chase data (●) and dTTP chase data (◆)] are shown. The linear [dTTP] dependence of the fast exponential rate constant provided a k_{on} of 0.07 ± 0.01 mM^{-1}·s^{-1} (slope) and a k_{off} of 0.4 ± 1.1 s^{-1} (*y* intercept).

of dTTP binding (k_{on}) of 0.07 ± 0.01 μM^{-1}·s^{-1} and a k_{off} of 0.4 ± 1.1 s^{-1}. The average amplitude of the first phase of the burst remained constant at 1.11 ± 0.21 sites per hexamer (Fig. 2*B*). The exponential rate constant and the amplitude of the second phase of the burst did not show a marked increase with [dTTP]. The average values of the amplitude and the rate constant at various [dTTP] were 0.95 ± 0.28 sites per hexamer and 0.2 ± 0.07 s^{-1}, respectively. Both the acid and chase experiments were repeated at several different 4A′ concentrations (0.083–5.0 μM hexamer concentration). The rate constants and the burst amplitudes were found to be independent of 4A′ concentrations in this range (data not shown), indicating that the observed kinetics were most likely not limited by 4A′ oligomerization.

The hydrolysis of one dTTP at a time or single-site hydrolysis of dTTP continues during steady-state dTTPase turnovers, as shown below. To measure the number of dTTPs/hexamer that are catalytically competent during steady state turnover, the following three-syringe rapid-quench-flow experiment was designed. In these experiments, 4A′ protein was mixed with [α-^{32}P]dTTP for 60 s to allow enzyme catalysis to reach steady state. At 60 s, excess nonradiolabeled dTTP was added, and the reactions were acid-quenched after varying chase times (10–60 s; see *Materials and Methods*). As shown in Fig. 3, only one dTTP per hexamer was converted to product

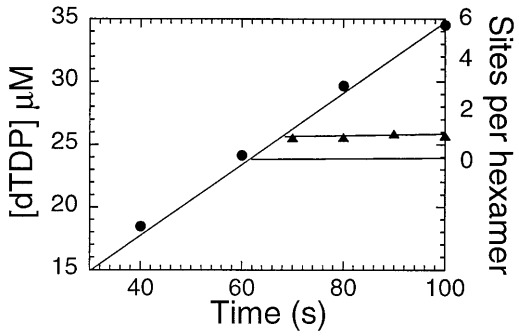

FIG. 3. Number of catalytically competent dTTPs bound to 4A′ during steady-state dTTPase turnover. In a three-syringe experimental set-up (*Materials and Methods*), 4A′ (2 μM hexamer) was mixed with [α-^{32}P]dTTP (150 μM) for 60 s. Nonradiolabeled dTTP (7 mM) was added at 60 s, and the reactions were chased for 10–60 s prior to acid-quenching. As shown (▲), only one additional dTTP per hexamer was hydrolyzed to dTDP during the chase period. When reactions were not chased, the steady state hydrolysis of [α-^{32}P]dTTP (150 μM) continues at 0.14 ± 0.006 s^{-1} (●).

during the chase period. These results are consistent with the pre-steady-state kinetic results and show that the hexamer has only one dTTP tightly bound at any time that is catalytically competent for hydrolysis.

The above pre-steady-state acid-quench and pulse–chase experiments suggest a dTTPase mechanism where binding and hydrolysis of dTTP occurs in a sequential manner, as shown in Fig. 4*A*. The key feature of the model is the cooperativity among the hexameric subunits that assures both the hydrolysis of only one dTTP at a time and the sequential binding and hydrolysis of dTTP at separate sites. The following results suggested that binding and hydrolysis of dTTP at separate sites are coupled events. First, the rate of second dTTP binding is close to the rate of first dTTP hydrolysis—i.e., the second dTTP is not bound tightly until the first dTTP has hydrolyzed. Thus, tightening of the second dTTP is coupled to the hydrolysis of the first dTTP. Second, although the first dTTP appears to have a tight K_d (k_{off}/k_{on} provided a range from close to 0 to 20 μM), the [dTTP] dependence of the acid-quench burst rate provided a $K_{1/2}$ that was much weaker (170 μM). The weak K_d may represent binding of a second dTTP. These results suggest that hydrolysis of the first dTTP may be dependent on the binding of the second dTTP. The proposed mechanism in Fig. 4*A* was verified by kinetic simulation (HOPKINSIM). The rate constants obtained from the fit to the pre-steady-state kinetic experiments were used as initial estimates in the simulation. As shown by the solid lines in Fig. 4 *B* and *C*, the mechanism and rate constants shown in Fig. 4*A* accurately predict both the acid-quench and pulse–chase kinetics.

The above experiments provide evidence for participation of only two dTTPase sites in the sequential mechanism. If the third site is participating in sequential catalysis, it cannot be distinguished because the kinetics enter steady state and information about the number of sites is lost. However, previous studies with a mutant helicase, 4A′/K318A, suggest likely participation of all 3 sites in catalysis (18). The K318A mutation in the P-loop of 4A′ allows dTTP binding, but the helicase is defective in dTTP hydrolysis. When 4A′/K318A was mixed with 4A′, the helicase and DNA-stimulated dTTPase activities of the mixed hexamer are greatly reduced, even with only one mutant subunit per hexamer. Thus participation of all sites seems essential for the helicase activity.

The dTTPase mechanism of T7 helicase cannot be compared with other hexameric helicases at the present time, since a detailed rapid acid-quench and pulse–chase pre-steady-state kinetic study of the NTPase activity has not been reported for

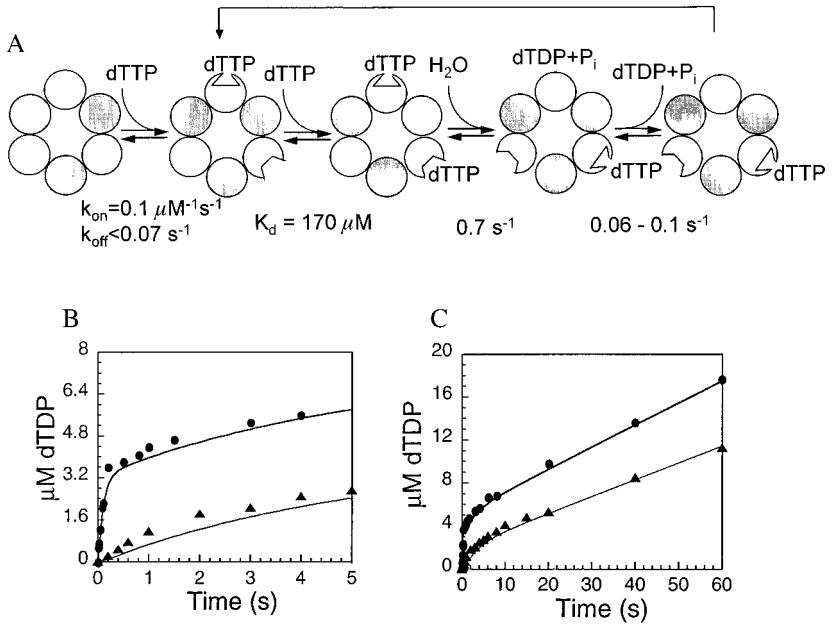

FIG. 4. Kinetic simulation of the sequential dTTP hydrolysis mechanism of 4A′. (*A*) Proposed mechanism of dTTP hydrolysis by 4A′ hexamer. (*B* and *C*) The acid-quench (▲) and pulse–chase (●) kinetics from Figs. 1 and 2 in different time windows. The solid lines in *B* and *C* are simulated curves created by HOPKINSIM using the mechanism and the rate constants shown in *A*. The sequential binding and hydrolysis of two dTTP and the conformational change that leads to tight binding of second dTTP were simulated as follows. The first dTTP binding was assumed to be tight and the second dTTP binding was assumed to be a rapid equilibrium step. Thus, the first dTTP in the E·$(TTP)_2$ species was fully chased to product but the second dTTP was not chased to product in the pulse–chase experiment. Because the second dTTP becomes tightly bound after hydrolysis of the first dTTP, the dTTP in the E·TDP·P_i·TTP species was chased to product in the chase experiment.

any other helicase. There are indications in the literature that the hexameric RuvB helicase may hydrolyze ATP with burst kinetics (19). The burst amplitude in an acid-quench type experiment was estimated to be close to 2 ATP/hexamer by extrapolation of steady-state kinetics to zero time. The difference in the burst amplitudes between 4A′ and RuvB suggests some differences in the NTPase kinetics of these helicases. However, a more detailed investigation of the NTPase kinetics is necessary to properly address any mechanistic differences in the NTPase kinetics of hexameric helicases. The dimeric *E. coli* helicase Rep, on the other hand, has been more thoroughly studied (3). Based on thermodymamic DNA binding studies (20), the investigators have proposed a model of helicase function in which the two subunits of the helicase alternate their affinity for ssDNA and dsDNA, depending on the state of the nucleotide bound to the subunit. All available data, therefore, suggest that cooperativity and coordination in DNA and NTP binding by the subunits of the helicase (dimeric or hexameric) is a central feature of the mechanism of action of helicases.

The Hexamer Has Three Noncatalytic Nucleotide Binding Sites. Previous dTTP binding studies have shown that 4A′ hexamer binds only 3–4 dTTPs with a high affinity at equilibrium (16). We wished to determine if the high-affinity sites were the ones involved in dTTP hydrolysis. An experiment was designed to measure how fast helicase-bound dTTPs exchanged with free dTTP in the medium. In this experiment, carried out in the absence of DNA, 4A′ protein was preincubated with [α-^{32}P]dTTP for 30 s. Excess nonradiolabeled dTTP was added as a chase, and the solution was passed through NC filters after varying chase times. Before chase was added (zero chase time), a total of 3.7 ± 0.87 nt were bound per hexamer (Fig. 5*A*). During the 30-s chase time, 1–2 nt dissociated rapidly from 4A′; yet surprisingly, the remaining 2–3 nt dissociated from 4A′ with a very slow rate constant of 0.008 ± 0.002 s^{-1} (Fig. 5*A*). These nucleotides exchanged about 20 times slower relative to the dTTPase turnover rate under the same conditions (0.36 s^{-1} at 10 mM dTTP). In other words, in the 400 s it took for the tightly bound nucleotides to dissociate, the 4A′ hexamer had undergone about 160 turnovers of dTTP hydrolysis. Clearly these sites are not participating in the dTTPase turnover; hence we refer to these sites as noncatalytic.

To determine the identity of the slowly exchanging nucleotides (dTTP or dTDP), the protein-bound nucleotides on the NC filter were extracted and analyzed by TLC. Before nonradiolabeled dTTP chase was added, of the 3.7 ± 0.87 nt bound, 20% were dTDP and the rest were dTTP (Fig. 5*B*). After nonradiolabeled dTTP chase was added, the slowly exchanging nucleotides were mostly dTTP (80–90%) and did not hydrolyze even after 30 min of reaction. Thus the noncatalytic sites may be designed to bind nucleotides tightly and not hydrolyze or hydrolyze very slowly. Interestingly, dTDP exchanged rapidly from the noncatalytic sites (Fig. 5*B*, lanes 10 and 11).

The dTTP bound at the noncatalytic sites can be replaced by dTMP-PCP with little effect on the dTTPase turnover rate constant. A similar exchange experiment as above with [α-^{32}P]dTMP-PCP showed that of the three tightly bound dTMP-PCP, 1.5–2 exchanged with free dTTP in the medium with a rate of 0.002 ± 0.0004 s^{-1} (Fig. 5*C*). One dTMP-PCP remained bound even after 1 h of incubation with dTTP chase. To determine if dTMP-PCP bound at the noncatalytic sites had any effect on the dTTPase turnover, 4A′ protein was preincubated with dTMP-PCP and dTTP hydrolysis was measured while dTMP-PCP was still bound to 4A′. Interestingly, the dTTPase turnover rate was only slightly lower than normal (most likely due to inhibition; K_i of dTMP-PCP is around 0.6 μM assuming competitive inhibition; data not shown), and there were no lags in the dTTPase kinetics (Fig. 5*C Inset*). These results show that dTMP-PCP nucleotides bound at the noncatalytic sites have little effect on the dTTPase turnovers at the catalytic sites.

There is evidence for two classes of nucleotide binding sites in *E. coli* DnaB (21) and *E. coli* rho protein (22). Equilibrium nucleotide binding studies have shown that these hexameric

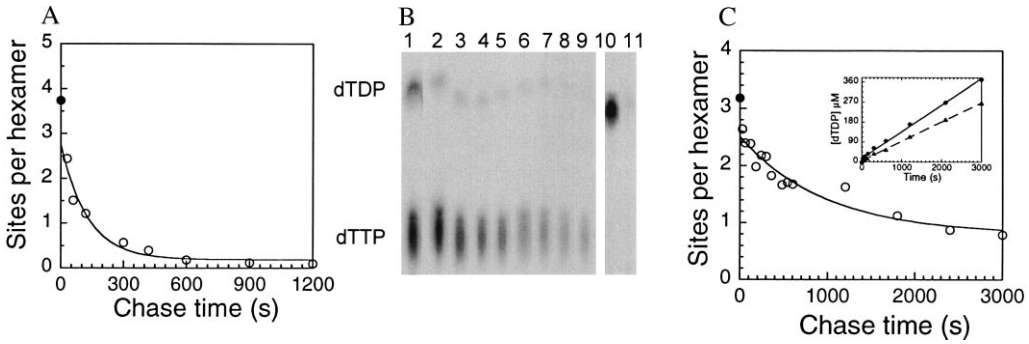

FIG. 5. Identification of 4A′-bound nucleotides and their dissociation kinetics. (*A*) 4A′ (2 μM hexamer) and [α-^{32}P]dTTP (200 μM) were mixed at 18°C for 30 s and nonradiolabeled dTTP (10 mM) was added at time zero. After varying chase times (30 s to 20 min), aliquots were filtered through NC membranes. A total of 3.7 ± 0.87 nt (error calculated from seven independent measurements) were bound to 4A′ at zero chase time (●). After addition of dTTP chase, the 2–3 4A′-bound nucleotides exchanged at 0.008 ± 0.002 s^{-1} (○). (*B*) To identity the tightly bound nucleotides, NC membranes were extracted and the eluted nucleotides were analyzed by polyethyleneimine-cellulose TLC. Here the PhosphorImager scan of the TLC plate is shown. Lane 1, dTDP (20%) and dTTP (80%) bound to 4A′ before chase was added. Lanes 2–9, nucleotides bound after 0.5, 3, 6, 9, 12, 15, 20, 25 min of chase. In all lanes, dTDP is 6–17% and dTTP is 94–83%. Lane 10, dTDP bound to 4A′ after 90 min of incubation. Lane 11, almost no dTDP remained bound after 30-s chase with unlabeled dTTP. (*C*) The exchange of 4A′-bound dTMP-PCP was measured by preincubating 4A′ (0.83 μM hexamer) with [α-^{32}P]dTMP-PCP (98 μM) and adding 5 mM dTTP as chase. Three to four dTMP-PCP are bound before chase was added (●). Two dTMP-PCPs exchanged with unlabeled dTTP in the medium (○) with a rate constant of 0.002 ± 0.0004 s^{-1}; one dTMP-PCP did not exchange even after 50-min chase time. (*Inset*) dTTP hydrolysis in the presence of dTMP-PCP. Reaction conditions were same as in *C*, except 4A′ was preincubated with dTMP-PCP and hydrolysis of 5 mM [α-^{32}P]dTTP was measured. dTTP was hydrolyzed without lag at 0.1 ± 0.001 s^{-1} in the presence of dTMP-PCP (▲) and at 0.14 ± 0.003 s^{-1} in the absence of dTMP-PCP (◆).

helicases bind 3 nt strongly and 3 nt weakly, but the significance of this result was not clear. Our results show that the strong nucleotide binding sites of 4A′ are noncatalytic sites, and dTTPs bound at these sites do not dissociate nor do they get hydrolyzed through many dTTPase turnovers. We propose that the three noncatalytic sites are located on alternating subunits of the hexameric ring. This is the simplest arrangement of the noncatalytic sites, and because of its intrinsic symmetry, it seems more likely than other possible arrangements. Future studies will address the role of the noncatalytic sites. However, we can speculate that these sites may be essential for hexamer stabilization, DNA binding, or promoting dTTP hydrolysis.

Rotational Catalysis and Comparison to the F_1-ATPase. This study has provided important insights into the mechanism of dTTP binding and hydrolysis by 4A′ helicase. Interestingly, our proposed mechanism shows remarkable similarity to the binding change mechanism of the F_1-ATPase. The F_1-ATPase is a component of the ATP synthase, which couples the energy of the proton motive force to ATP synthesis during oxidative phosphorylation. The two enzymes also share structural similarities. F_1-ATPase is a $\alpha_3\beta_3$ hexamer with six ATP binding sites, of which three are noncatalytic and three are catalytic sites (11, 23). 4A′ has six identical subunits, thus the catalytic and the noncatalytic sites must result from induced asymmetry due to oligomerization or dTTP binding.

We compare here the sequential mechanism of dTTP hydrolysis by 4A′ to the binding change mechanism of the ATP synthase (Fig. 6). In ATP synthase, it is the proton-motive-force that drives ATP synthesis, whereas in 4A′, it is the energy from dTTP hydrolysis that drives DNA translocation. One of the central features of the binding change mechanism is cooperative catalysis among the three active sites as shown by oxygen-18 exchange and by pre-steady state ATPase and ATP synthesis kinetic experiments (23). This mechanism allows tight binding of substrates (ADP + P_i) and release of product

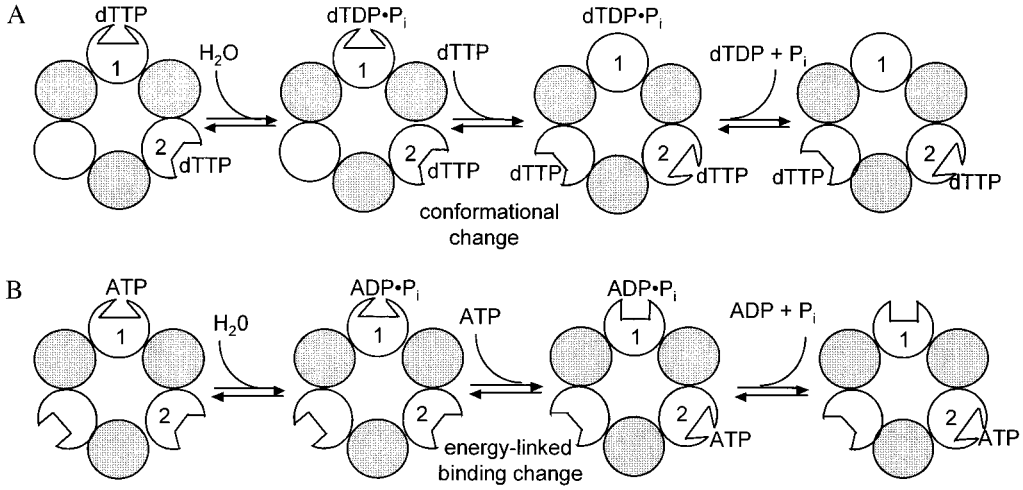

FIG. 6. Comparison of the sequential mechanism of dTTP hydrolysis by 4A′ (*A*) to the binding change mechanism of the ATP synthase (*B*). The shaded subunits in both enzymes depict noncatalytic sites. The catalytic sites are differentiated as "tight" (number 1) or "loose" (number 2) in the furthest left hexamer. In 4A′, we start with a single catalytic site in the "tight" conformation (number 1). The other catalytic sites in 4A′ interact weakly with dTTP that rapidly exchanges with free dTTP in the medium. The tightening of dTTP at the second site accompanies the conformational change step that occurs either directly before, concurrently with, or directly after, dTTP hydrolysis at the first site. The example here shows the conformational change occurring directly after hydrolysis at the first site.

(ATP) to occur simultaneously at separate catalytic sites on the synthase. This is much like what we propose for 4A′ based on pre-steady-state kinetic experiments. As shown in Fig. 6, the hydrolysis of dTTP at the first catalytic site on 4A′ is analogous to the synthesis of ATP from ADP + P_i at the first catalytic site on the synthase. The conformational change that occurs after dTTP hydrolysis tightens the interactions of the substrate (dTTP) at the second catalytic site, and at the same time weakens the interaction of products (dTDP + P_i) at the first site. This step is analogous to the binding change conformational change in the synthase that causes tightening of substrates (ADP + P_i) at the first site and release of product (ATP) at the second site. The last step in this single-turnover mechanism, the dissociation of products (dTDP + P_i) from the first catalytic site on 4A′, is analogous to the binding of substrates (ADP + P_i) to the first catalytic site.

Even though we have examined the dTTP hydrolysis mechanism in the absence of DNA, the discovery of the similarities to the F_1-ATPase represents a major advance in understanding the action of helicases. This is because of the wealth of mechanistic information available on the F_1-ATPase that may be applied to hexameric helicases. Previous studies have shown that 4A′ hexamer binds ssDNA through the central hole (8), and other hexameric helicases such as DnaB, *E. coli* RuvB, and simian virus 40 T antigen may also bind DNA through the central hole (24–26). The γ subunit of F_1 can be considered analogous to the DNA and it also binds in the central hole of F_1-ATPase. In fact, in the proposed structural alignment between 4A′ and the F_1-ATPase (12), the proposed DNA binding site of 4A′ aligns with the loop of the F_1-ATPase that interacts with the γ subunit. In 4A′ and DnaB helicases, the ssDNA interacts specifically with one subunit, and the state of the nucleotide modulates the interactions with the DNA (9, 24, 27). If dTTP binding and hydrolysis facilitate ssDNA binding and release, then the sequential catalysis would promote sequential binding and release of ssDNA from one site to another on the hexamer. Such movement of the ssDNA, with respect to the subunits of the 4A′ hexamer, may be analogous to the rotation of the γ subunit with respect to the F_1 ring (28, 29). The rotation of γ with respect to the F_1 ring, brought about by proton translocation, has been proposed to modulate the interaction of nucleotides at the catalytic sites. In helicases, sequential NTP hydrolysis at the catalytic sites can bring about rotation of the hexameric ring with respect to the ssDNA, which could promote unidirectional translocation along ssDNA or passing of the dsDNA through the ring helicases such as RuvB and T antigen.

Unidirectional translocation along ssDNA can be the basis for dsDNA unwinding. Several studies in the literature support the idea that 4A′, DnaB, and T4 gp41 helicases bind to only one ssDNA of the fork substrate (8, 9, 27) (perhaps the lagging strand) through the central hole (30, 31) and exclude the other ssDNA (the leading strand) from the hole. With this mode of DNA binding, duplex DNA unwinding can be brought about by unidirectional translocation of the helicase along the lagging strand and displacement of the leading ssDNA tail excluded from the hole.

This research was supported by American Cancer Society Grant NP832A and National Institutes of Health Grant GM55310.

1. Lohman, T. M. (1992) *Mol. Microbiol.* **6,** 5–14.
2. Lohman, T. M. (1993) *J. Biol. Chem.* **268,** 2269–2272.
3. Lohman, T. M. & Bjornson, K. P. (1996) *Annu. Rev. Biochem.* **65,** 169–214.
4. West, S. C. (1996) *Cell* **86,** 177–180.
5. Subramanya, H. S., Bird, L. E., Brannigan, J. A. & Wigley, D. B. (1996) *Nature (London)* **384,** 379–383.
6. Bernstein, J. A. & Richardson, C. C. (1988) *Proc. Natl. Acad. Sci. USA* **85,** 396–400.
7. Patel, S. S. & Hingorani, M. M. (1993) *J. Biol. Chem.* **268,** 10668–10675.
8. Egelman, E. H., Yu, X., Wild, R., Hingorani, M. M. & Patel, S. S. (1995) *Proc. Natl. Acad. Sci. USA* **92,** 3869–3873.
9. Hingorani, M. M. & Patel, S. S. (1993) *Biochemistry* **32,** 12478–12487.
10. Miwa, Y., Horiguchi, T. & Shigesada, K. (1995) *J. Mol. Biol.* **254,** 815–837.
11. Abrahams, J. P., Leslie, A. G. W., Lutter, R. & Walker, J. E. (1994) *Nature (London)* **370,** 621–628.
12. Washington, M. T., Rosenberg, A. H., Griffin, K., Studier, F. W. & Patel, S. S. (1996) *J. Biol. Chem.* **271,** 26825–26834.
13. Story, R. M., Weber, I. T. & Steitz, T. A. (1992) *Nature (London)* **355,** 318–325.
14. Yu, X. & Egelman, E. H. (1997) *Nat. Struct. Biol.* **4,** 101–104.
15. Patel, S. S., Rosenberg, A. H., Studier, F. W. & Johnson, K. A. (1992) *J. Biol. Chem.* **267,** 15013–15021.
16. Hingorani, M. M. & Patel, S. S. (1996) *Biochemistry* **35,** 2218–2228.
17. Johnson, K. A. (1992) in *The Enzymes*, ed. Sigman, D. S. (Academic, Orlando, FL), Vol. 20, pp. 1–61.
18. Patel, S. S., Hingorani, M. M. & Ng, W. M. (1994) *Biochemistry* **33,** 7857–7868.
19. Marrione, P. E. & Cox, M. M. (1995) *Biochemistry* **34,** 9809–9818.
20. Wong, I. & Lohman, T. M. (1992) *Science* **256,** 350–355.
21. Bujalowski, W. & Klonowska, M. M. (1993) *Biochemistry* **32,** 5888–5900.
22. Geiselmann, J. & von Hippel, P. H. (1992) *Protein Sci.* **7,** 850–860.
23. Boyer, P. D. (1993) *Biochim. Biophys. Acta* **1140,** 215–250.
24. Bujalowski, W. & Jezewska, M. J. (1995) *Biochemistry* **34,** 8513–8519.
25. Stasiak, A, Tsaneva, I. R., West, S. C., Benson, C. J. B., Yu, X. & Egelman, E. H. (1994) *Proc. Natl. Acad. Sci. USA* **91,** 7618–7622.
26. Mastrangelo, I. A., Hough, P. V. C., Wall, J. S., Dobson, M., Dean, F. B. & Hurwitz, J. (1989) *Nature (London)* **338,** 658–662.
27. Yu, X., Hingorani, M. M., Patel, S. S. & Egelman, E. H. (1996) *Nat. Struct. Biol.* **3,** 740–743.
28. Sabbert, D. & Junge, W. (1996) *Nature (London)* **381,** 623–625.
29. Noji, H., Yasuda, R., Yashida, M. & Kinosita, K., Jr. (1997) *Nature (London)* **386,** 299–302.
30. Yong, Y. & Romano, L. J. (1996) *Chem. Res. Toxicol.* **9,** 179–187.
31. Raney, K. D., Carver, T. E. & Benkovic, S. J. (1996) *J. Biol. Chem.* **271,** 14074–14081.